NOAA Technical Report

Visible Infrared Imaging Radiometer Suite (VIIRS) Imagery Environmental Data Record (EDR) User's Guide

Version 1.1

Washington, D.C.
27 December 2013
Revised: 29 April 2014

U.S. DEPARTMENT OF COMMERCE
National Oceanic and Atmospheric Administration
National Environmental Satellite, Data, and Information Service

NOAA TECHNICAL REPORTS

NOAA Technical Report

Visible Infrared Imaging Radiometer Suite (VIIRS) Imagery Environmental Data Record (EDR) User's Guide

Version 1.1

Curtis Seaman[1], Donald Hillger[2], Thomas Kopp[3], Ryan Williams[4], Steven Miller[1] and Daniel Lindsey[2]
[1]Colorado State University/CIRA
Fort Collins, CO 80523
[2]NOAA/NESDIS/Satellite Applications and Research
Fort Collins, CO 80523
[3]The Aerospace Corporation
Los Angeles, CA 90009
[4]NASA/GSFC
Greenbelt, MD 20771

Washington, DC
April 2014

Revision History

Revision	Date	Brief Summary of Changes
Version 0.9(draft)	12 December 2013	Baseline document draft
Version 1.0	27 December 2013	Baseline document
Version 1.1	29 April 2014	Updated Section 3 to reflect changes made to GDNBO files beginning in May 2014; minor update to Section 7 re: Wisconsin Direct Broadcast data

Table of contents

Contents

1. Introduction

The Visible Infrared Imaging Radiometer Suite (VIIRS) was first launched aboard the Suomi National Polar-orbiting Partnership (S-NPP) satellite on 28 October 2011. S-NPP was the first satellite launched as part of the Joint Polar Satellite System (JPSS) program. JPSS, a joint NOAA and NASA program, was designed to develop and launch the next generation of polar orbiting satellites to follow NOAA's Polar-orbiting Earth Observing System (POES) program.

The VIIRS instrument was designed to combine and, where possible, improve upon the best characteristics of the Moderate-resolution Imaging Spectroradiometer (MODIS), the Advanced Very-High Resolution Radiometer (AVHRR), the Sea-viewing Wide Field-of-view Sensor (SeaWIFS) and the Operational Linescan System (OLS). VIIRS is one of five scientific instruments aboard S-NPP and is responsible for the "Key Performance Parameter" (KPP) of Imagery for the JPSS program.

VIIRS data is distributed in two primary forms: Sensor Data Records (SDRs), which may be considered Level-1 products, and Environmental Data Records (EDRs), which may be considered Level-2 products, using NASA terminology. SDRs contain the calibrated radiance, reflectance and/or brightness temperature data and other data collected by the instrument (e.g. geolocation information). There are a variety of EDRs produced operationally, ranging from land and ocean surface properties to cloud and aerosol properties. These may or may not use ancillary data, but are all based on SDR data. In this document, the focus is on the Imagery EDRs, which contain the calibrated radiance, reflectance and/or brightness temperature data that has been remapped to a Ground-Track Mercator (GTM) projection. Differences in imagery produced from SDRs and EDRs will be discussed. It is important to note that the information supplied in this document applies only to Imagery EDRs. Not all EDRs use the GTM projection, but all Imagery EDRs do. However, the information provided for the display of images based on SDR data may be useful for the display of other EDR products that have not been remapped to the GTM grid.

This document is designed to serve the following purposes: introduce the VIIRS instrument, provide a quick reference point for information found in various VIIRS Algorithm Theoretical Basis Documents (ATBD) related to using VIIRS Imagery data, discuss common issues users may (or will) encounter in the use of VIIRS Imagery data and products, and present information useful to individual users or organizations interested in processing and/or archiving VIIRS Imagery data.

More detailed information on the VIIRS instrument and VIIRS Imagery data and products may be found in NOAA Technical Report NESDIS 142 (VIIRS SDR User's Guide; Cao et al. 2013a) or in the ATBDs referenced (see Section 9).

2. The VIIRS instrument

VIIRS is a "whiskbroom" radiometer. The instrument is sensitive to 22 wavelength bands (channels) ranging in central wavelength from 0.412 μm to 12.01 μm on the electromagnetic spectrum (Table 1). Five of the bands are designated as "High-resolution Imagery Bands", also referred to as "I-bands". Sixteen of the bands are designated as "Moderate Resolution Bands", also referred to as "M-bands". The "Day/Night band" (DNB) is panchromatic, sensitive to visible and near-infrared (NIR) wavelengths ranging from daylight down to the low levels of radiation observed at night. The spatial resolution of the instrument at viewing nadir is approximately 375 m for the I-bands and 750 m for the DNB and M-bands (Table 1). Note that the native resolution is not identical in the along-track and across-track directions. The instrument has a field-of-view of 112.56° in the across-track direction. With a nominal altitude of 824 km, this field-of-view corresponds to a swath-width of approximately 3060 km, which is wide enough to provide complete coverage of the globe, with no data gaps near the Equator.

Table 1. VIIRS channels.

Band number/gain	VIIRS wavelength (μm)	VIIRS nadir pixel size along track × cross track (km)	Primary application
M1, dual	0.412	0.742 × 0.259	Ocean color, aerosols
M2, dual	0.445	0.742 × 0.259	Ocean color, aerosols
M3, dual	0.488	0.742 × 0.259	Ocean color, aerosols
M4, dual	0.555	0.742 × 0.259	Ocean color, aerosols
I1, single	0.640	0.371 × 0.387	Imagery, vegetation
M5, dual	0.672	0.742 × 0.259	Ocean color, aerosols
M6, single	0.746	0.742 × 0.776	Atmospheric correction
I2, single	0.865	0.371 × 0.387	Vegetation
M7, dual	0.865	0.742 × 0.259	Ocean color, aerosols
DNB, multiple	0.7	0.742 × 0.742	Imagery
M8, single	1.24	0.742 × 0.776	Cloud particle size
M9, single	1.38	0.742 × 0.776	Cirrus cloud cover
M10, single	1.61	0.742 × 0.776	Snow fraction
I3, single	1.61	0.371 × 0.387	Binary snow map
M11, single	2.25	0.742 × 0.776	Clouds
M12, single	3.70	0.742 × 0.776	Sea surface temperature (SST)
I4, single	3.74	0.371 × 0.387	Imagery, clouds
M13, dual	4.05	0.742 × 0.259	SST, fires
M14, single	8.55	0.742 ×0.776	Cloud-top properties
M15, single	10.76	0.742 × 0.776	SST
I5, single	11.45	0.371 × 0.387	Cloud imagery
M16, single	12.01	0.742 × 0.776	SST

From Lee et al. (2006).

S-NPP is located in a sun-synchronous orbit with an equator crossing time of 13:30 local time (LT). As a result, VIIRS provides complete coverage of the globe twice daily: once in the early afternoon (ascending overpass) and once in the early morning hours (descending overpass). As the satellite travels from the Equator toward the poles, overlap between successive orbits increases such that locations near the left edge of one scan, for example, may be imaged on the right edge of scan on the successive orbit. The orbital period of S-NPP is approximately 101 minutes. The 3060 km-wide swath and orbital period combine to provide quasi-geostationary temporal coverage at and near the poles.

VIIRS channels are numbered in order of increasing wavelength (except the Day/Night Band). Figure 1 shows the nominal relative spectral response (RSR) functions for the visible and NIR bands (M1 through M11 and I1 through I3). Figure 2 shows the RSR functions for the mid- and long-wave infrared bands (M12 through M15, I4 and I5). Figure 3 shows the RSR function for the Day/Night Band. For comparison purposes, Figures 1 and 2 show the RSR functions for the associated AVHRR channels, and Figure 3 shows the RSR for the low-light visible channel of the OLS.

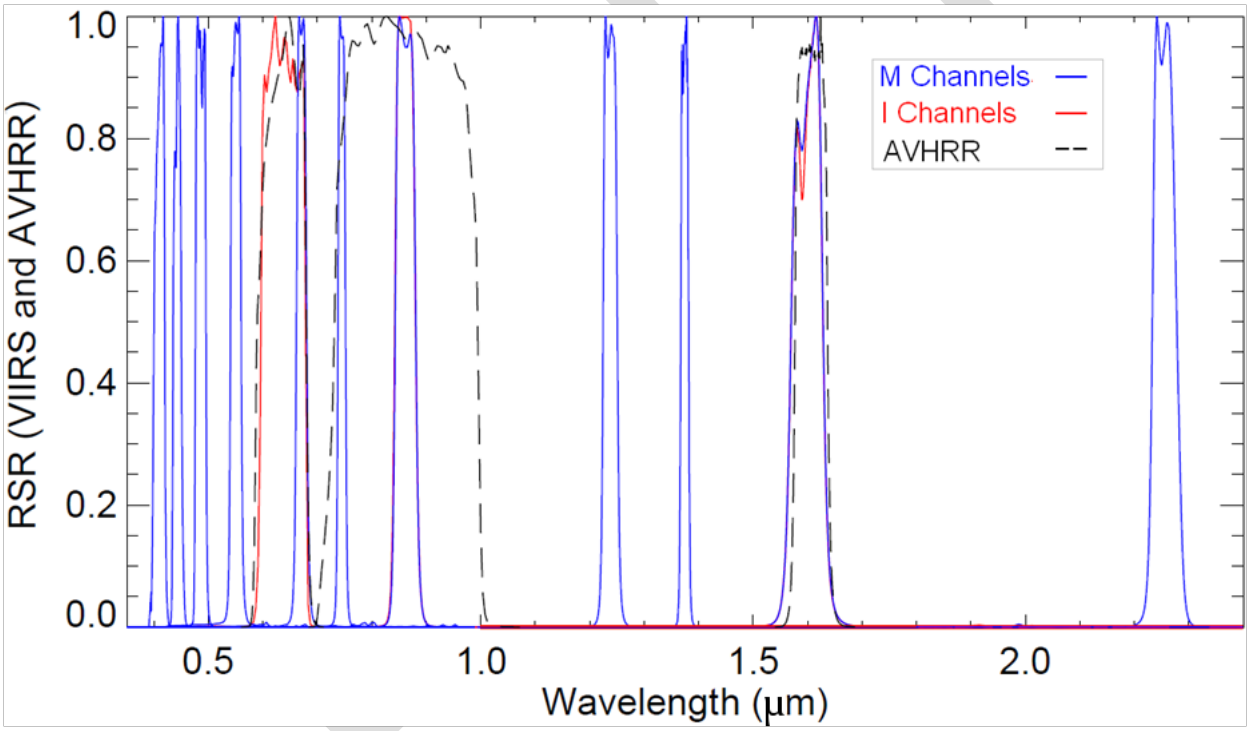

Figure 1. Nominal Relative Spectral Response (RSR) functions for the VIIRS M-bands 1-11 (blue), I-bands 1-3 (red) and associated bands from AVHRR (black dashed). From Cao et al. (2013a).

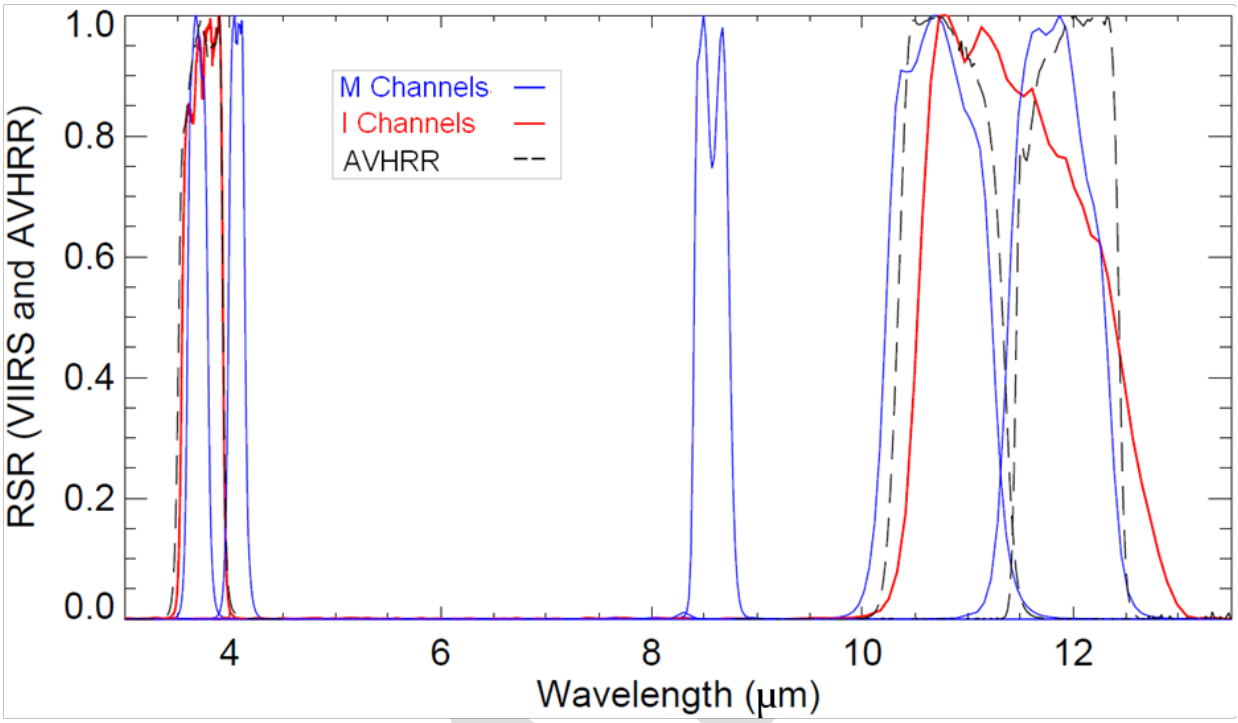

Figure 2. Same as Figure 1, except for VIIRS M-bands 12-15 (blue), I-bands 4 and 5 (red), and associated bands from AVHRR (black dashed). From Cao et al. (2013a).

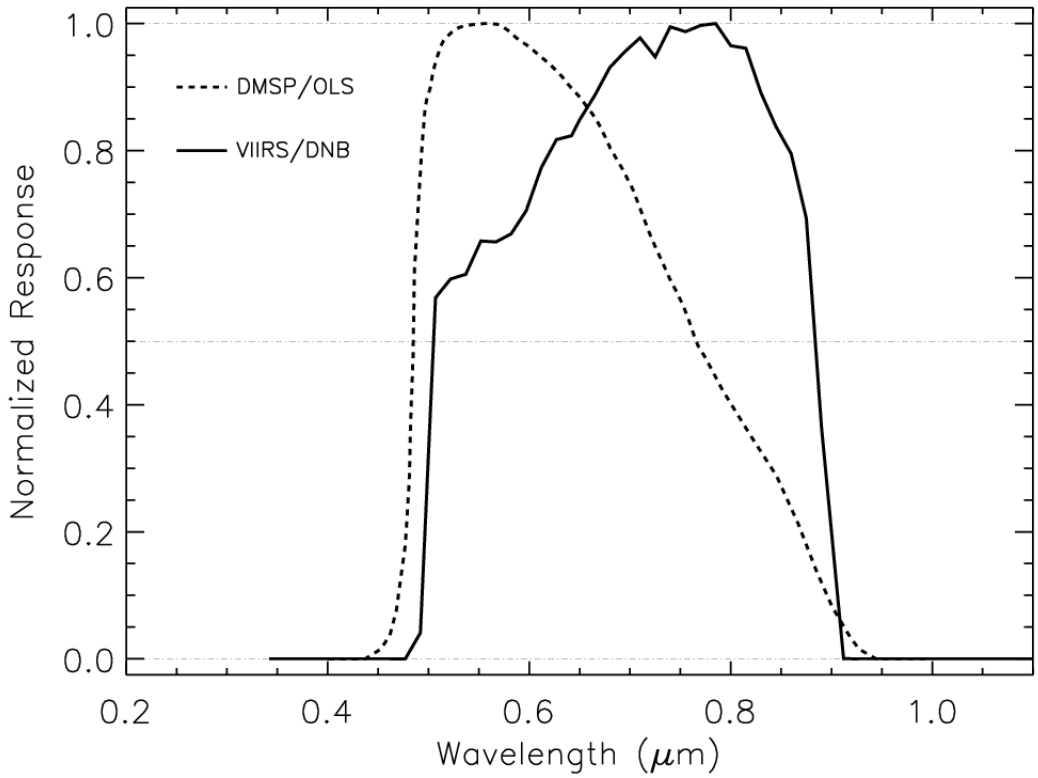

Figure 3. Nominal Relative Spectral Response functions for the VIIRS Day/Night Band (solid) and the low-light visible channel from OLS (dashed). From Miller et al. (2013b).

3. VIIRS Imagery Data Files

The raw data collected by the VIIRS instrument is recorded as Raw Data Records (RDRs), a Level-0 product using NASA nomenclature. The RDR files are produced from the data that are transmitted to Earth and received by NOAA (or other satellite ground stations including field terminals with an appropriate antenna). The raw data is calibrated and processed (converted from photon counts to radiance, reflectance and/or brightness temperature) and written to Sensor Data Records (SDR) data files. At the same time, geolocation information contained in the RDR files is written to separate SDR geolocation files. This data is broken up into segments referred to as "granules".

As the satellite moves through space, a constantly rotating mirror reflects incoming radiation onto a set of detectors. One revolution of the mirror is one scan. The M-bands and Day/Night Band use 16 detectors (16 rows of pixels per scan) while the I-bands use 32 detectors (32 rows of pixels per scan) with twice the spatial resolution. At nadir, the width of each scan is approximately 12 km. Therefore, each scan of the instrument produces a strip of Earth-viewing data 12 km x 3060 km (ignoring bow-tie effects, which will be discussed in detail in Section 4). It takes approximately 1.79 seconds to complete each scan, during which time the instrument views the Earth for approximately 0.56 seconds. The amount of time it takes to complete one scan is such that the sub-satellite point moves the width of each scan, eliminating any unviewed portions of the Earth's surface between scans. A collection of 48 consecutive scans comprise one granule. As a result, each granule represents approximately 86 seconds of data, and covers an area approximately 570 x 3060 km in size (again, ignoring bow-tie effects).

Table 2: VIIRS Imagery file types.

SDRs

- Geolocation files:
  - GITCO, GMTCO, GIMGO, GMODO, GDNBO
- I-band Data files:
  - SVI01, SVI02, SVI03, SVI04, SVI05
- M-band Data files:
  - SVM01, SVM02, SVM03, SVM04, SVM05, SVM06, SVM07, SVM08, SVM09, SVM10, SVM11, SVM12, SVM13, SVM14, SVM15, SVM16
- DNB Data file:
  - SVDNB

EDRs

- Geolocation files:
  - GIGTO, GMGTO, GNCCO
- I-band Data files:
  - VI1BO, VI2BO, VI3BO, VI4BO, VI5BO
- M-band Data files*:
  - VM01O, VM02O, VM03O, VM04O, VM05O, VM06O
- NCC Data file:
  - VNCCO

* Unlike other Imagery EDRs, the M-band data files are not numbered according to the SDR data they contain. See page 14.

In order to minimize file sizes, data is generally distributed as individual granules[1]. The calibrated data for each channel (extracted from the RDR files) are written to a separate SDR file for each granule, as are the geolocation data. Currently, the SDR data from the Day/Night Band, the five I-bands, and a set of six M-bands, along with the geolocation information are further processed (remapped) to the Ground-Track Mercator grid, and written to EDR files. For each granule, there are 42 Imagery files currently produced (see Table 2): 5 SDR + 3 EDR geolocation files, 10 I-band data files (5 SDR + 5 EDR), 22 M-band data files (16 SDR + 6 EDR) and two files for the Day/Night Band (1 SDR plus an EDR product referred to as Near Constant Contrast [NCC]). Each of these files is saved in Version 5 of the Hierarchical Data Format (HDF-5). These 42 files for each granule total approximately 2 GB of data (see Table 3), and 1012 granules are produced each day.

VIIRS files use a consistent file naming convention. The file name includes the file type, satellite identifier, date, start and end time of the granule, orbit number, file creation time, and the source of the file. An example is shown in Figure 4.

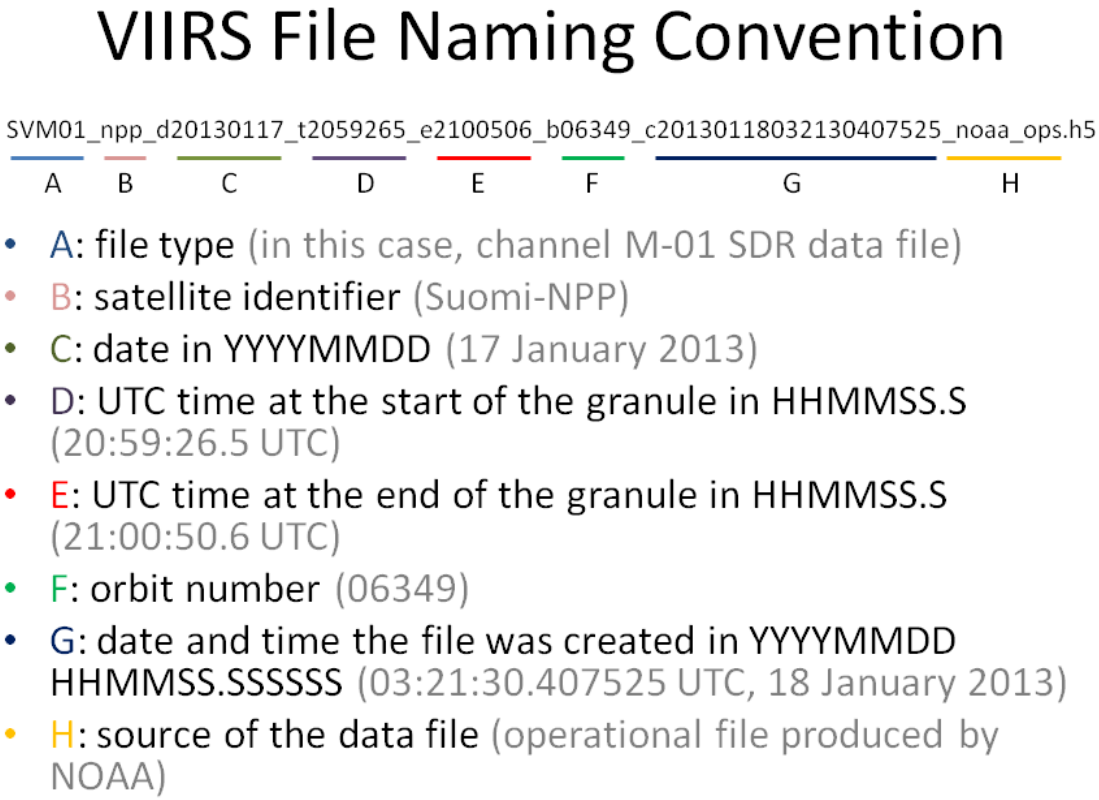

Figure 4. The VIIRS file name convention.

[1] NOAA's Comprehensive Large Array-data Stewardship System (CLASS), one of the primary sources of VIIRS data (see Section 7), will, by default, aggregate granules in groups of four into a single file unless the user specifies de-aggregation. Geolocation data is also aggregated with data files, unless specified, which may result in prohibitively large files for some users.

I-band and M-band SDR data files have two types of geolocation files associated with them. The first type projects the instrument lines of sight onto the WGS84 ellipsoid. The second type accounts for the parallax effects of terrain using a digital elevation model and are referred to as "terrain corrected". Prior to May 2014, the Day/Night Band SDR geolocation was not terrain corrected and was only available for the WGS84 ellipsoid. Due to demand from the user community, terrain corrected geolocation information was produced for the Day/Night Band beginning in May 2014. Rather than create an additional file type, the determination was made to provide both the ellipsoid and terrain corrected geolocation information inside the GDNBO files. This has increased the typical file size for GDNBO files. Some data sources (see Section 7) only provide terrain corrected geolocation files for the M- and I-band data.

The EDR geolocation files, including the Near Constant Contrast geolocation, all use the Ground-Track Mercator projection grid, which is not terrain corrected.

The eight geolocation file types are distinguished as follows:

- GDNBO: DNB SDR WGS84 ellipsoid geolocation (and terrain-corrected geolocation for files produced after May 2014)
- GIGTO: I-band EDR Ground-Track Mercator geolocation
- GIMGO: I-band SDR WGS84 ellipsoid geolocation
- GITCO: I-band SDR terrain corrected geolocation
- GMGTO: M-band EDR Ground-Track Mercator geolocation
- GMODO: M-band SDR WGS84 ellipsoid geolocation
- GMTCO: M-band SDR terrain corrected geolocation
- GNCCO: DNB EDR (Near Constant Contrast; NCC) Ground-Track Mercator geolocation

This information is summarized in Table 4.

Table 3. Approximate file sizes of the VIIRS Imagery file types for a single granule.
* GDNBO file sizes were increased beginning in May 2014 to accommodate both ellipsoid and terrain corrected geolocation information. See text.

File Type	File Size (approximate)
SDRs	
GIMGO	309 MB
GITCO	210-250 MB
GMODO	77 MB
GMTCO	50-60 MB
GDNBO	85-90 MB/130-160 MB*
SVI (01, 02, 03)	40 KB (night) 25-30 MB (day)
SVI04	20-25 MB
SVI05	25-30 MB
SVM (01, 02)	40 KB (night) 7-8 MB (day)
SVM (03, 04, 05)	40 KB (night) 11 MB (day)
SVM06	40 KB (night) 6-7 MB (day)
SVM07	5 MB (night) 11 MB (day)
SVM (08, 10, 11)	660 KB (night) 6-8 MB (day)
SVM09	40 KB (night) 2-5 MB (day)
SVM12	4-8 MB
SVM13	11-12 MB
SVM (14, 15, 16)	6-7 MB
SVDNB	10-11 MB
EDRs	
GIGTO	423 MB
GMGTO	106 MB
GNCCO	136 MB
VI (1, 2, 3) BO	26 KB (night) 60 MB (day)
VI (4, 5) BO	60 MB
VM (01, 02, 03) O	24 KB (night) 12 MB (day)
VM (04, 05, 06) O	12 MB
VNCCO	9 MB

Every geolocation file contains the following information for each pixel: latitude, longitude, height, satellite azimuth angle, satellite zenith angle, solar azimuth angle, solar zenith angle, and range to satellite. For the non-terrain corrected geolocation files, "height" corresponds to the geoid height above ellipsoid. For the terrain corrected geolocation files, "height" corresponds to the surface elevation above mean sea level (MSL). Heights and distances are reported in meters, while angles are reported in degrees. In addition, the DNB and NCC geolocation files contain the lunar azimuth and lunar zenith angles. The EDR geolocation files - including NCC - also include two additional arrays that keep track of the row and column indices of the SDR pixel that was mapped to the given EDR pixel location within the array.

Data arrays in the SDR and EDR files match the size of the arrays within the associated geolocation files. These array sizes are as follows: 6400 x 1536 for the I-band SDR files, 3200 x 768 for the M-band SDR files, 4064 x 768 for the DNB (SDR) files, 8241 x 1531 for the I-band EDR files, and 4121 x 771 for the M-band EDR files and the NCC (EDR) files.

Referring back to Table 3, it is apparent that file sizes vary by file type even between those that have the same array size. This is due to variations in the way the data is stored within the HDF-5 format. Data arrays (radiance and reflectance or brightness temperature) may be stored as either 16-bit unsigned integers or 32-bit floating point numbers. Most geolocation information is stored as 32-bit floating point numbers. Data arrays stored as floating point values are stored in the proper scientific units. Data stored as unsigned integers must be converted to the proper scientific units using the scale and offset values provided as a separate array. For example, to read in an unsigned integer array of radiance values and convert the values to the proper units, one must read in the "Radiance" data array and the "RadianceFactors" data array. The scale factors are always two-element vectors of 32-bit floating point values, where the first value is the "scale" and the second value is the "offset". If we represent the "RadianceFactors" data array as the vector [c_0, c_1], where c_0 is the scale and c_1 is the offset, then the floating point value (in proper scientific units), f, is related to the given unsigned integer value, n, by the equation:

$$f = c_0 n + c_1$$

Error fill values will depend on whether or not the data is stored as unsigned integers or floating point values, as will be discussed later in this section.

Unless otherwise specified, radiance values are given in units of W m^{-2} sr^{-1} μm^{-1}. Radiance values for the Day/Night Band are band-integrated and have units of W cm^{-2} sr^{-1}. Reflectance values are unitless. Brightness temperature values are given in units of K. Within the metadata, times are given as either a character string in HHMMSS format using Coordinated Universal Time (UTC) or are recorded as a 64-bit unsigned integer, which is a count of the number of microseconds since 00:00:00 UTC on 1 January 1958.

There is one SDR data file type for each VIIRS channel, and each SDR data file contains the calibrated radiance data. Channels in the visible and NIR wavelengths (where solar reflectance dominates the received signal), except for the DNB, also contain reflectance values calculated from the radiances; these are the channels that are shown in Figure 1 (M1 through M11 and I1 through I3). Mid- and longwave infrared channel data files (where thermal emission from the Earth's surface dominates the signal) report brightness temperatures in lieu of reflectance values; these are the channels that are shown in Figure 2 (M12 through M15, I4 and I5). The

DNB files only contain radiance values for reasons that will be discussed in Section 6. This is summarized in Table 5.

At the time of this writing, Imagery EDR data files comprise only a subset of the VIIRS channels. Operationally, only 6 M-band SDRs are converted to EDRs. All five I-band SDRs are converted to EDRs and the DNB is converted to the Near Constant Contrast (NCC) EDR. The NCC EDR contains reflectance only (see Section 6). The I-band EDR data files are numbered according to the input SDR data; these files contain radiance (all files), reflectance (VI1BO, VI2BO and VI3BO) and brightness temperature (VI4BO and VI5BO). The M-band EDRs do not use the same numbering system as the input SDR data. They are instead referred to as the 1st, 2nd, 3rd, etc. EDRs. These files contain data arrays named "Radiance" and "BrightnessTemperatureOrReflectance". The values in the BrightnessTemperatureOr Reflectance array will be either brightness temperature or reflectance based on the input SDR data (see Table 5).

The software used to produce M-band EDR data files was designed to be flexible such that any set of 6 M-band SDRs may be converted to EDRs. The lowest number channel from the SDR data will be the 1st EDR, and so on. Each M-band EDR file has a metadata item located within the HDF-5 structure named "Band_ID" that contains the input M-band channel number. There is currently a mandate within the JPSS program that M14, M15 and M16 data must be produced as EDRs operationally, leaving only the first three M-band EDRs flexible.

As of this writing, the default M-band EDR types are as follows:

- VM01O contains SVM01 data
- VM02O contains SVM04 data
- VM03O contains SVM09 data
- VM04O contains SVM14 data
- VM05O contains SVM15 data
- VM06O contains SVM16 data

Users are encouraged to locate the "Band_ID" metadata item for verification. The location of this item is found at '/Data_Products/VIIRS_Mxxx_EDR/VIIRS_Mxxx_GRAN_0/Data_ID/' within the HDF-5 data structure, where 'xxx' may have the value of 1ST, 2ND, 3RD, etc.

There has been demand from the user community to produce EDR files from all 16 M-band SDR files. The feasibility of this is currently under investigation. It is likely that only 6 M-band EDRs will be available until the launch of the JPSS-1 satellite, at the earliest.

Table 6 provides a list of error fill values used in all VIIRS SDR and EDR data. These fill values depend on whether the data is stored as 16-bit unsigned integers or 32-bit floating point numbers. The most commonly encountered fill values when displaying VIIRS Imagery are "N/A", "OBPT" and "VDNE". With the exception of M-10 and the DNB, visible and NIR channel data is not produced at night. In this case, the data arrays will contain either "N/A" fill or "VDNE" fill. "OBPT" fill is found in all SDR data files, where overlapping pixels are removed due to the "bowtie effect". This is discussed in more detail in the next section.

Table 4. List of geolocation files based on the WGS84 ellipsoid and parallax-corrected for the effects of terrain.

Ellipsoid Geolocation Files		Terrain Corrected Geolocation Files
GMODO	**GIGTO**	**GITCO**
GIMGO	**GMGTO**	**GMTCO**
GDNBO*	**GNCCO**	**GDNBO***

* As of May 2014, GDNBO files contain both the ellipsoid and terrain-corrected geolocation. Prior to this, only the ellipsoid geolocation was available. See text.

Table 5. List of VIIRS SDR files containing reflectance and brightness temperature. All SDR files contain radiance values. SVDNB files contain only radiance values.

SDR Files Containing Reflectance		SDR Files Containing Brightness Temperature	
SVI01	**SVM05**	**SVI04**	**SVM12**
SVI02	**SVM06**	**SVI05**	**SVM13**
SVI03	**SVM07**		**SVM14**
SVM01	**SVM08**		**SVM15**
SVM02	**SVM09**		**SVM16**
SVM03	**SVM10**		
SVM04	**SVM11**		

Table 6: VIIRS error fill values

Name	Description	Value	
		16-bit unsigned integer	32-bit floating point
N/A	Not applicable	65535	-999.9
MISS	Required value missing at time of processing	65534	-999.8
OBPT	Onboard pixel trim - overlapping pixel removed during SDR processing	65533	-999.7
OGPT	On-ground pixel trim – overlapping pixel removed during EDR processing	65532	-999.6
ERR	Error occurred during processing or non-convergence of solution	65531	-999.5
ELINT	Ellipsoid intersect failed – the instrument line-of-sight does not intersect the Earth's surface	65530	-999.4
VDNE	Value does not exist; processing algorithm did not execute	65529	-999.3
SOUB	Scaled over or under bounds – value not within allowed range	65528	-999.2

4. VIIRS and the Bow-Tie Effect

The VIIRS instrument has a constant angular resolution throughout each scan. The projection of this angle onto the surface below results in a continuously varying spatial resolution. Figure 5 shows a simplistic schematic of the phenomenon, which is exaggerated due to the curvature of the Earth. As a result, the finest spatial resolution occurs at instrument nadir and the coarsest spatial resolution occurs at the edge of the scan. This is true of any scanning instrument in space. As the resolution degrades away from nadir, the width of the scan in the along-track direction increases. Each scan, therefore, has the shape of a bow-tie and the effect on the data is referred to as the "bow-tie effect".

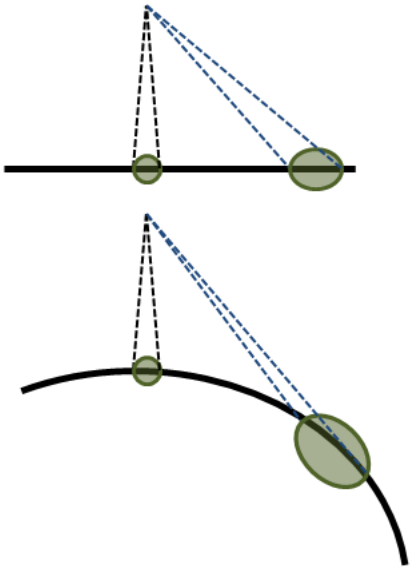

Figure 5. A schematic representation of the bow-tie effect. As the instrument, with constant angular resolution, scans away from nadir, the area of the Earth's surface within that field-of-view increases (as represented by the green ovals). This effect is exacerbated by the curvature of the Earth's surface.

VIIRS uses unique processing to reduce the "bow-tie effect". Note that the across-track and along-track resolutions are not identical at nadir (Table 1). During the processing from RDR to SDR, pixels are aggregated in the across-track direction in three distinct modes based on scan angle to create a more uniform spatial resolution (also called horizontal sampling interval, or HSI). This is shown in Figure 6. Without aggregation, the I-band and M-band across-track spatial resolution would degrade by approximately a factor of 6 between nadir and scan edge. With aggregation, the spatial resolution degrades by approximately a factor of 2, which is similar to the degradation in resolution in the along-track direction. The DNB uses a more vigorous pixel aggregation scheme that produces a nearly constant spatial resolution across the swath.

For comparison purposes, Figure 7 shows the nominal spatial geometries of VIIRS I-band pixels in relation to AVHRR, OLS and the MODIS 0.5 km-resolution channels. M-band pixels are a factor of 2 larger in the along-track and across-track dimensions than what is shown in Figure 7. The aggregation scheme used with VIIRS reduces distortion of the pixels, in addition to reducing the degradation in resolution caused by the bow-tie effect.

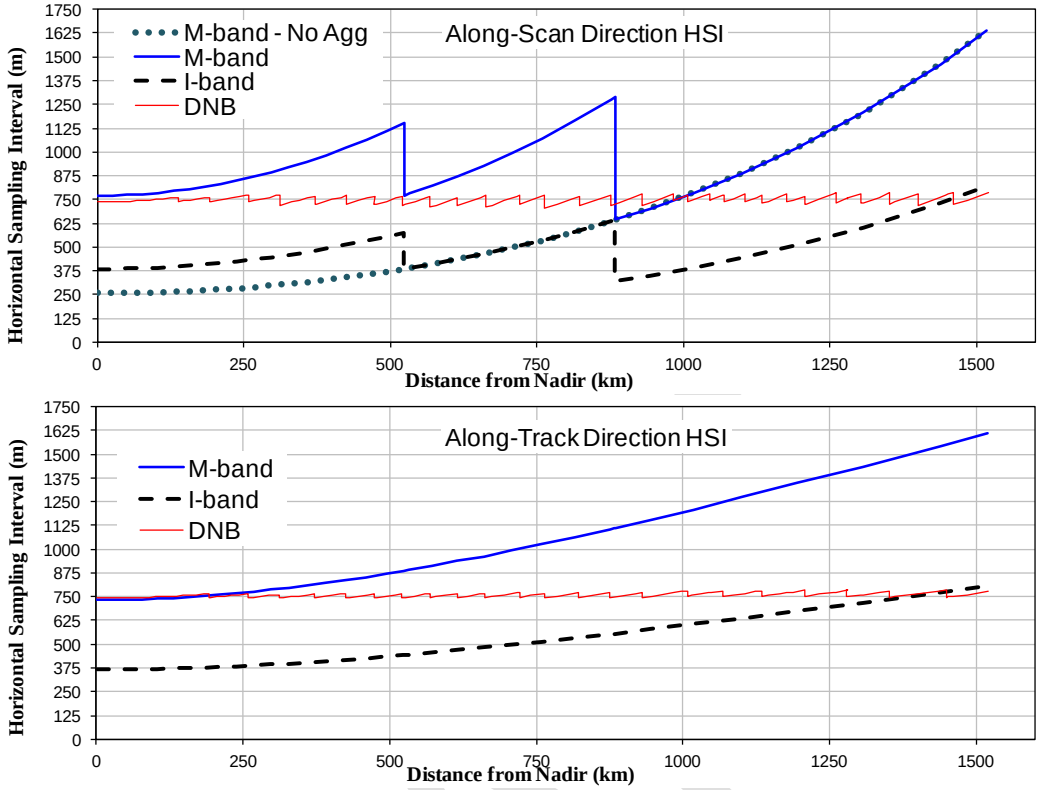

Figure 6. Horizontal sampling interval (HSI) of the VIIRS bands in the across-track direction (top) and along-track direction (bottom). In the top figure, the M-band HSI without aggregation (No Agg) is shown for comparison. From Cao et al. (2013).

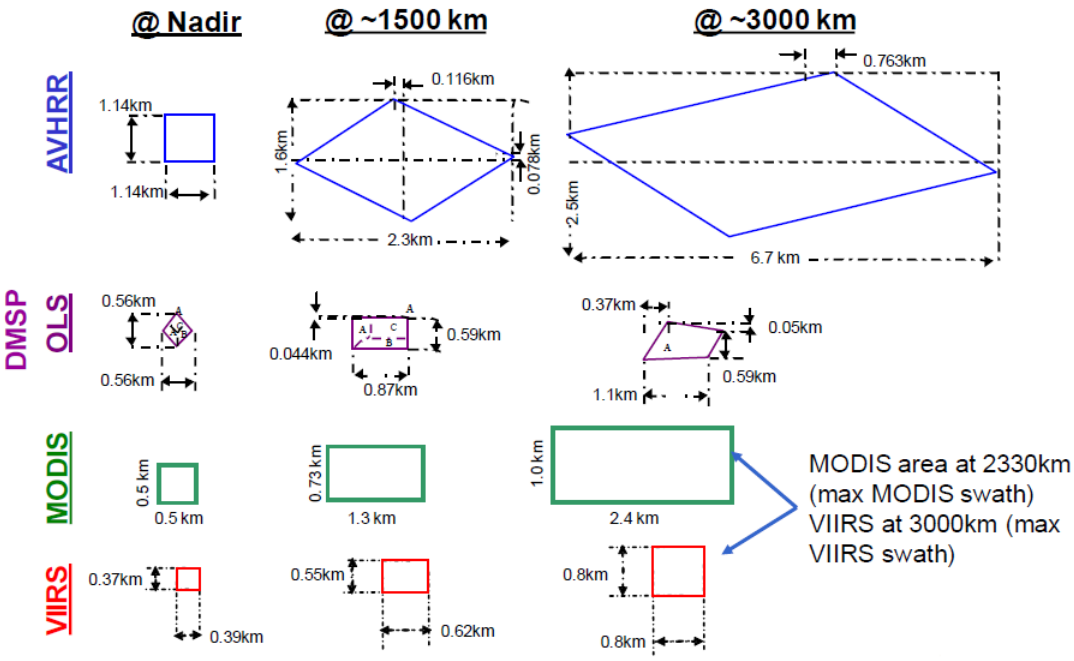

Figure 7. Nominal pixel geometries at nadir, 1500 km from nadir and near scan edge for AVHRR, OLS, MODIS (0.5 km-resolution channels) and VIIRS (I-bands). The vertical dimension represents the along-track direction. The horizontal dimension represents the across-track direction. From Miller et al. (2013a).

A schematic of the half-scan (from nadir to scan edge) for the M-bands is shown in Figure 8. The schematic for the I-bands is similar, except that the number of pixels is a factor of 2 greater. Without the bow-tie effect, each half-scan would be represented by the blue shaded area. Pixels outside the blue shaded area are pixels that overlap with the adjacent scan. Data values in pixels that are shaded red are deleted during the creation of the RDR files and are replaced with the OBPT fill value (Table 6) in the SDR files. These "bow-tie deletions" only occur in the data files. SDR geolocation files maintain their data within the bow-tie deletion lines.

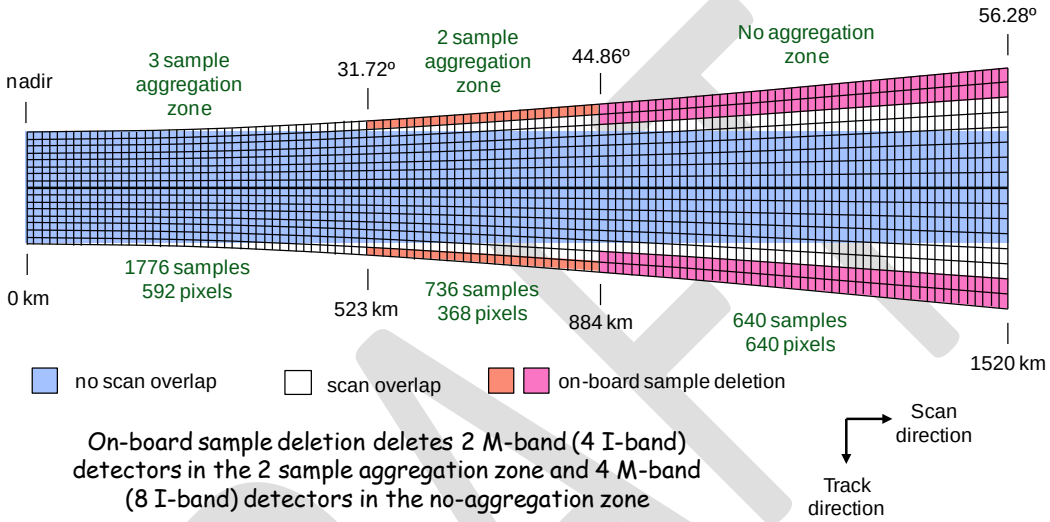

Figure 8. Schematic of VIIRS scan/pixel geometry from nadir to scan edge. The scale in the along-track direction has been exaggerated. Values above the image indicate the viewing angle of the instrument. The number of pixels shown in each aggregation zone (below the image) applies to single gain M-bands (see Table 1). Multiply these numbers by two for the I-bands. From Cao et al. (2013).

Proper display of the SDR data involves additional processing by the user to remove the bow-tie deletion lines. Figure 9 shows an example of imagery produced in the SDR data array space (without mapping to the Earth's surface). Bow-tie deletion lines show up as black in this image. Figure 10 shows the same image mapped to the Earth's surface using special processing to remove the bow-tie deletion lines. This image was created using IDL (Interactive Data Language) software, where the terrain-corrected geolocation was used to identify the OBPT fill values and replace them with the average value of the adjacent non-fill pixels. Other methods may produce more favorable results, depending on the application.

Notice in Figure 8 that there are pixels that overlap adjacent scans that are not given the OBPT fill value. This may create artifacts in the display of imagery that has not been properly mapped to the Earth's surface. Figure 11 shows two views of the same hurricane eye: one in data array space (unmapped) and one that has been mapped to the Earth's surface. This hurricane eye was observed off-nadir but before the start of the bow-tie deletion lines. Close inspection of the unmapped image reveals lines where pixels from adjacent scans overlap (indicated by the red arrows). When the image is mapped to the Earth's surface, these lines disappear. This is a plotting issue, and not an issue with the data.

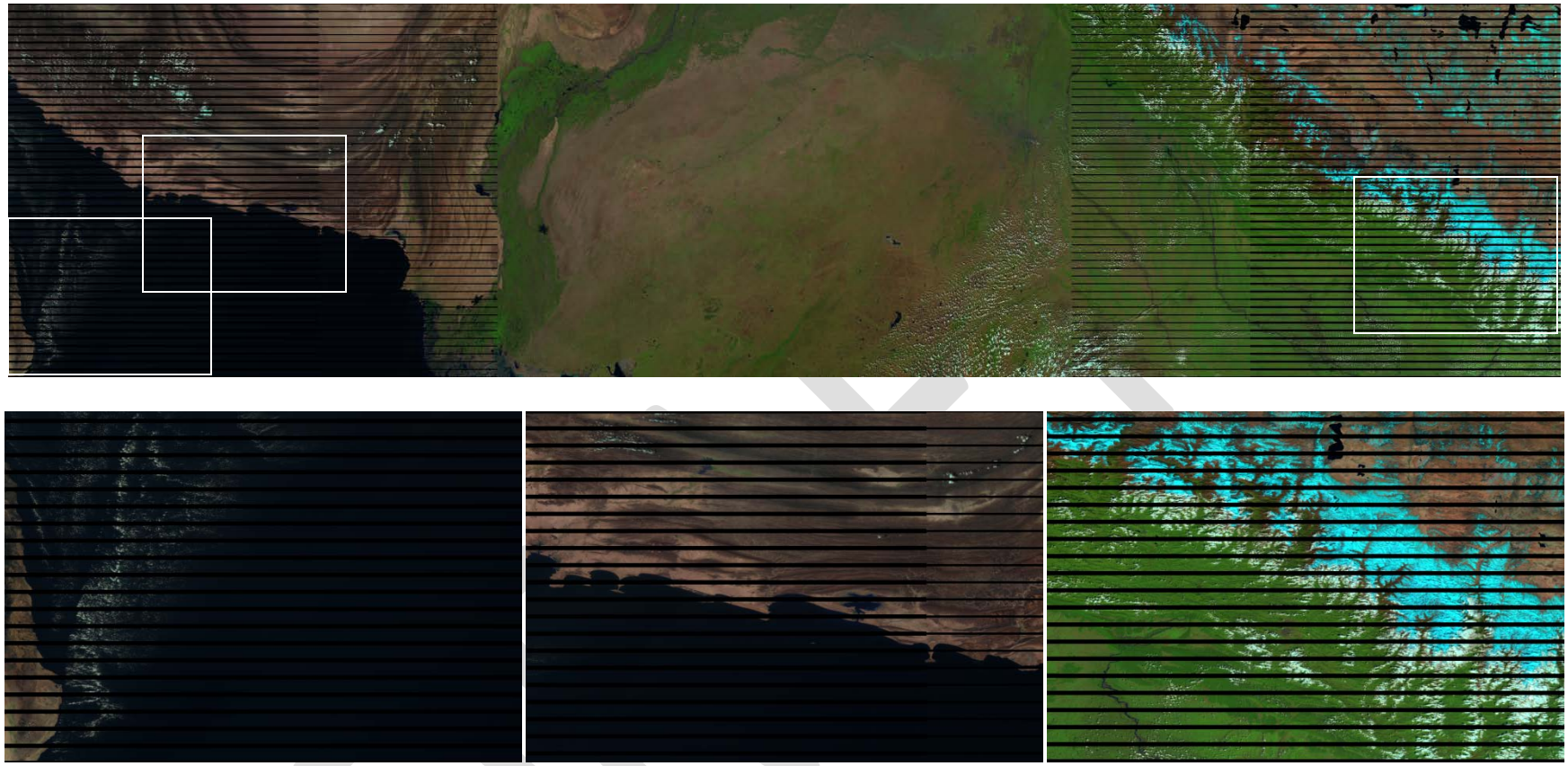

Figure 9. Example of an image created in SDR data array space. Top: RGB composite of channels I1, I2 and I3 from the granule at 08:14:37.9 UTC 24 October 2013, showing the full granule. The bow-tie deletion lines appear black in this composite. Bottom: zoomed in on the three outlined insets indicated by the white boxes, showing the impact of the bow-tie effect (and bow-tie deletions) on the SDR data arrays. Notice the repetition in various coastline, mountain and cloud features due to overlap between pixels of adjacent scans.

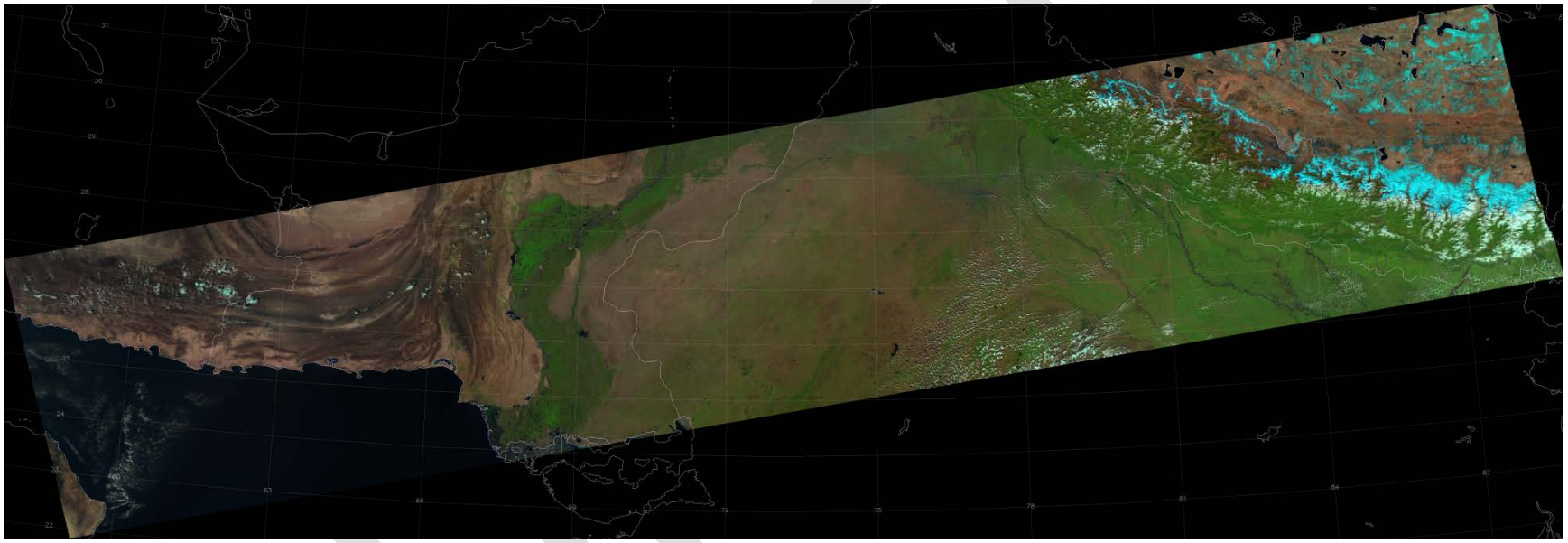

Figure 10. The same data as Figure 9 mapped to a projection of the Earth's surface using the terrain-corrected geolocation information with bow-tie deletion lines filled as discussed in the text. Notice the ragged edge on the east (right) edge of the scan, due to parallax effects caused by the Himalayas. This is properly accounted for in the terrain-corrected geolocation.

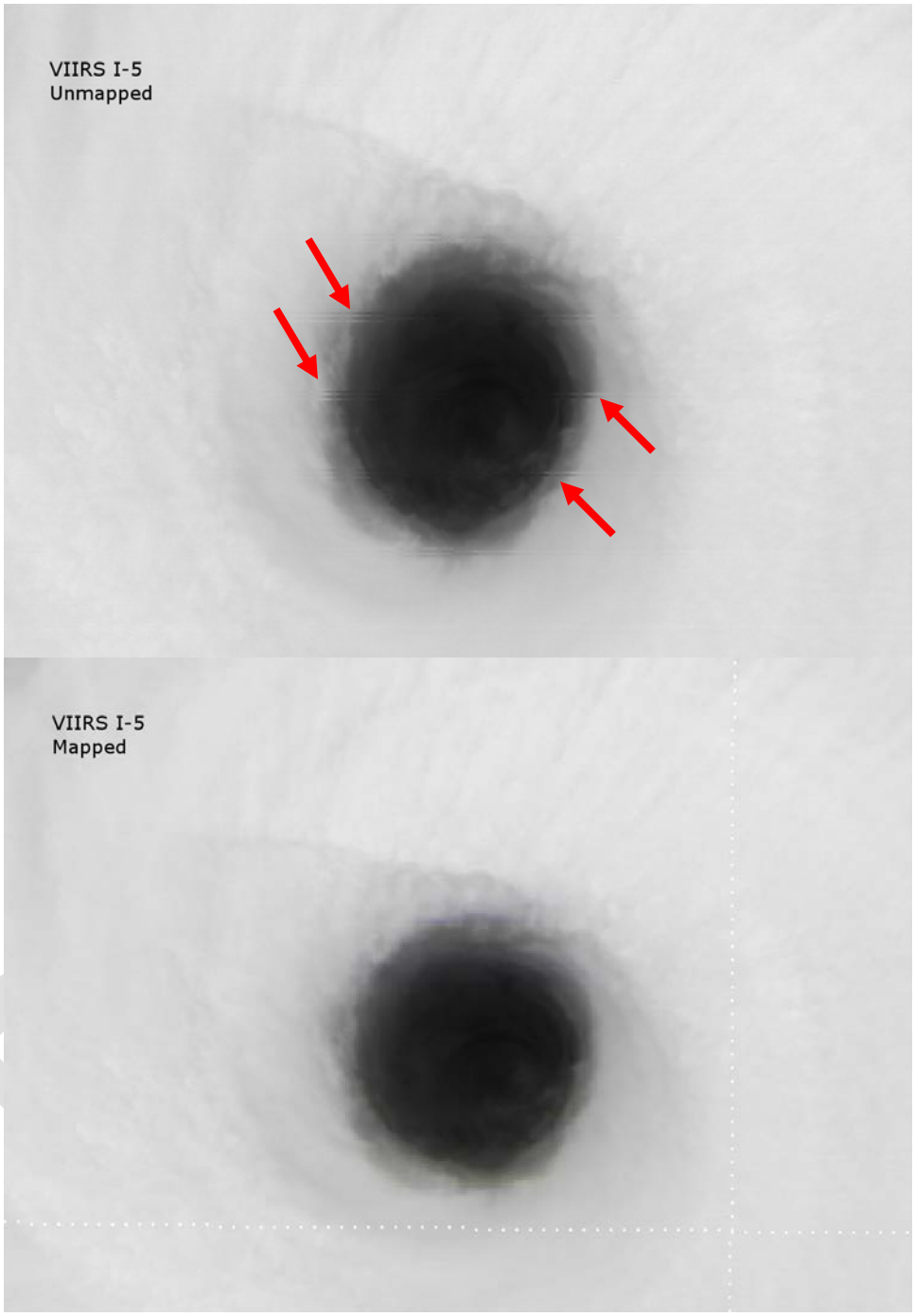

Figure 11. Example of a hurricane eye seen in an I5 SDR data granule. Top: The eye as seen in data array space (without mapping). Lines appear where pixels from adjacent scans overlap (indicated by the red arrows). Bottom: The same eye as seen projected onto the Earth's surface (with mapping using the geolocation information). Note that the eye appears more circular in the mapped image. This is due to the fact that the along-track and across-track resolution are not identical, although display of the unmapped image forces them to be. The geolocation information properly accounts for this in the mapped image.

Some satellite data are distributed with sub-sampled geolocation information (e.g. McIDAS Area files) and the geolocation of a particular pixel is to be interpolated from the sample of known latitude/longitude pairs and the known pixel resolution. As the VIIRS geolocation files contain the latitude and longitude of every pixel (even in bow-tie deletion lines), and the pixels are not necessarily spatially contiguous within the data arrays, users of VIIRS data are discouraged from trying to interpolate between pixels based on a sub-set of points when displaying SDR data.

Also note that, as the DNB is aggregated to maintain nearly constant horizontal spatial resolution across the swath, there is minimal overlap between scans. DNB data does not contain bow-tie deletion lines and OBPT and OGPT fill values should never be encountered when processing or displaying DNB data.

5. Imagery EDRs and the Ground Track Mercator Projection

The primary purpose of the Imagery EDRs is to provide VIIRS Imagery files with no visible artifacts caused by the bow-tie effect. To accomplish this, the SDR data is remapped onto what is referred to as the Ground Track Mercator (GTM) grid. The GTM grid represents a Mercator projection relative to the satellite. The GTM grid has constant horizontal spatial resolution in both the along-track and across-track directions, with the rows and columns of the data array orthogonal to one another, and the data is organized in a spatially contiguous manner within the data arrays. The I-band EDRs use 375 m resolution; the M-band and NCC EDRs use 750 m resolution

Although not always apparent in the display of SDR data, the path of each scan is not orthogonal to the satellite motion vector. This is shown by the schematic in Figure 12. It is a result of the constant motion of the satellite. The sub-satellite point of S-NPP moves at approximately 6.7 km s^{-1}. Recall from Section 3 that during each scan, the instrument views the Earth for approximately 0.56 seconds. That means the sub-satellite point travels in the along-track direction approximately 3.75 km between the start and end of the Earth-viewing portion of each scan. The constant rotation of the mirror combines with the constant motion of the satellite to mark out a line that is not orthogonal to the direction of the satellite's motion. If the bow-tie effect did not exist, each SDR granule would have the shape of a parallelogram rather than a rectangle. The EDR granules, in contrast, would have the shape of a rectangle.

Figure 13 shows this apparent "rotation" between the EDR granule and the associated SDR granule. Because of this apparent rotation, data from three consecutive SDR granules are required to produce one EDR granule. Data in the lower-left corner of each EDR file is provided by the previous SDR granule. Data in the upper-right corner is provided by the subsequent SDR granule. An EDR file that is produced when the previous or subsequent SDR granules are unavailable (or incomplete) will contain a triangular shaped region of MISS fill value (Table 6) in the appropriate corner of the data array. Prior to VIIRS Imagery achieving "Beta" quality status, this was a common problem with the use of EDR data. By delaying processing until all three SDR

granules are available (or reprocessing when an input SDR granule is repaired or completed), this problem has been fixed for the EDR files released operationally by NOAA. However, it may still be an issue for EDR files produced from Direct Download SDR data. EDR geolocation files are unaffected by these "missing triangles" as the definition of the GTM grid does not depend on the availability of the SDR data.

Figure 14 provides another example of the apparent rotation between an EDR granule and the associated SDR granule as projected onto a map of the Earth's surface. Note the cloud features in the upper-right corner of the EDR granule that are not present in the SDR granule, as well as cloud features in the lower-right of the SDR granule that are not visible in the EDR granule.

Users should note that the start and end times in the EDR filenames do not exactly match the start and end times in the SDR filenames (see Figure 4) for the associated granules. The start and end times are based on the time the instrument is viewing at nadir during the first and last scans included in the granule. As the EDR granules use data from the previous and subsequent granules, they have an earlier start time and later end time, in addition to having a different creation time.

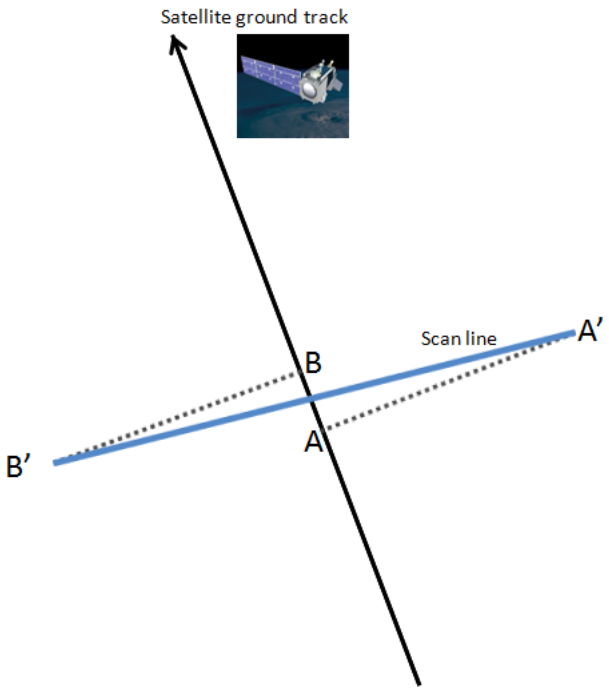

Figure 12. Schematic showing the lack of orthogonality between VIIRS scan lines and the along track direction. At the start of the scan, the satellite is above the point A on the Earth's surface, at which time the instrument is viewing the point A' at the edge of the scan. The line connecting points A and A' is perpendicular to the along-track direction. By the time the instrument mirror has rotated to view the point B' at the opposite edge of the scan, the satellite has moved over the point B. The line connecting points A' and B' (the scan line) is not perpendicular to the satellite ground track.

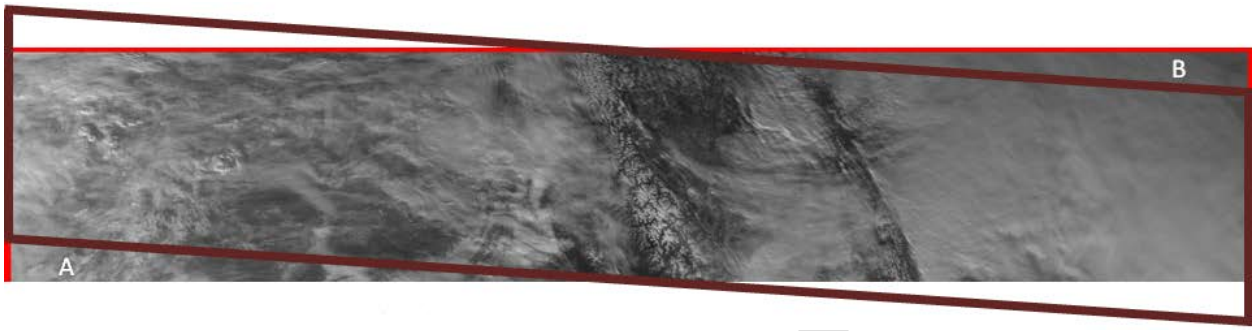

Figure 13. The background image shows an example of the 1st M-band EDR in data array space for a single granule (start time: 20:59:14.0 UTC 17 January 2013). The brown parallelogram outlines where the associated SDR file would spatially match up with the EDR granule, if it were overlaid. The lower-left corner of the EDR image (A) is comprised of data from the previous SDR granule. The upper-right corner of the image (B) is comprised of data from the subsequent SDR granule. Red pixels indicate N/A fill value (see text).

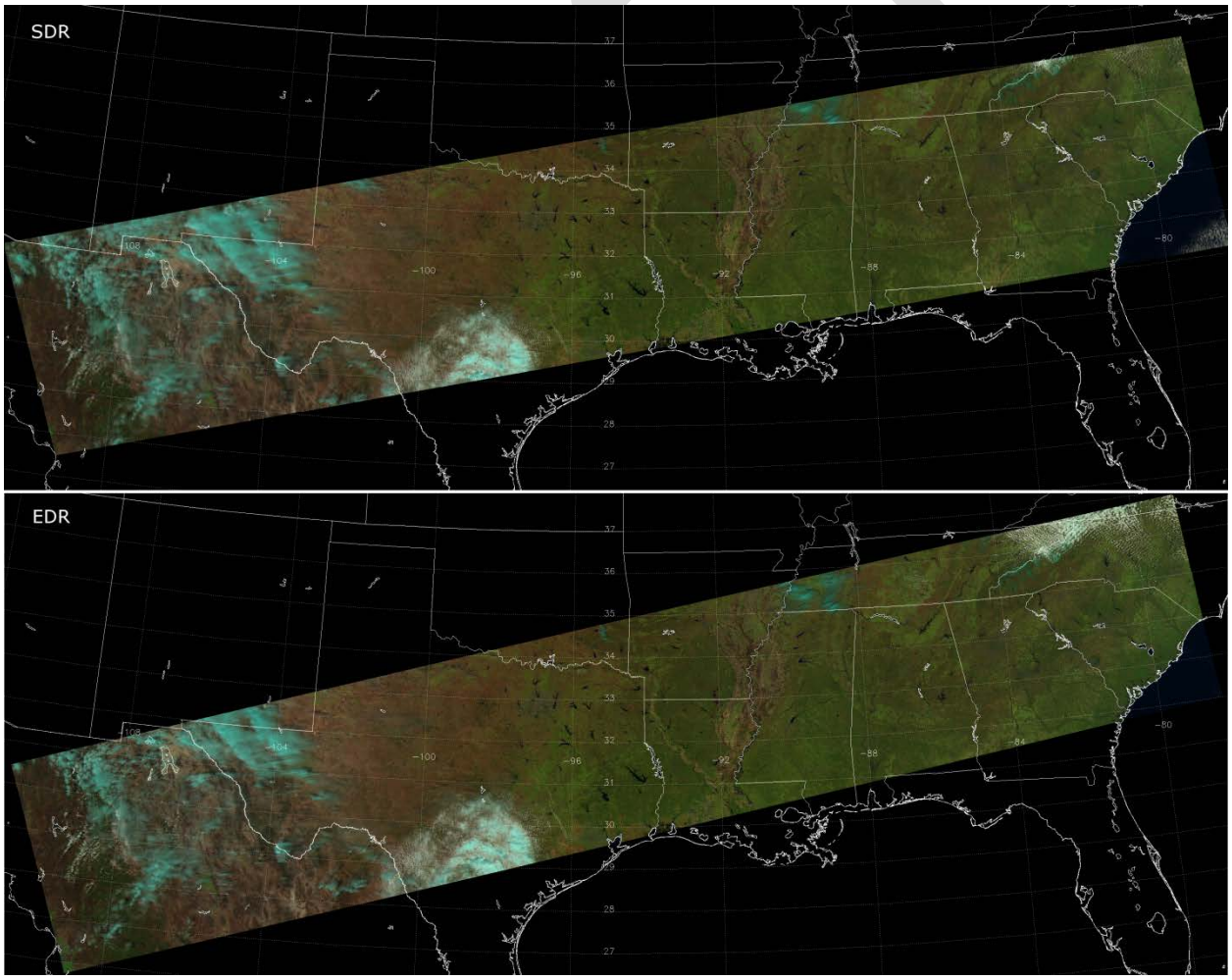

Figure 14. Top: RGB composite of I1, I2 and I3 SDR data for a single granule from 19:20:03.3 UTC 27 March 2013. Bottom: The same RGB composite using the I1, I2 and I3 EDR data for the associated granule (19:19:49.1 UTC 27 March 2013).

The procedure used to map SDR data onto the GTM grid is as follows. The data from the three required SDR granules is located. The scan with the closest center point to each GTM grid point is identified, along with the previous and subsequent scans. From these scans, an "interpolation rectangle" is identified. The interpolation rectangle is a 20x20 box of resolution-interpolated Earth locations (latitude and longitude pairs from the SDR geolocation files) that surround the GTM grid point. The latitude/longitude point within the interpolation rectangle that is closest to the GTM grid point (and that is not within the bow-tie deletion lines) is identified, and the array index values are saved. The SDR data values (radiance, reflectance and/or brightness temperature) from that point within the array are copied over to the array indices of that GTM grid point in the EDR file. There is a check to ensure the location of the closest SDR pixel is within a specified distance of the GTM grid point (based on the instrument viewing angle and, hence, nominal resolution of the SDR pixels). If there is no SDR pixel within the specified distance, the EDR pixel at that GTM grid point is set to N/A fill (Table 6).

As the data is copied (with no averaging or manipulation) from the SDR latitude/longitude to the latitude/longitude of the GTM grid point, a simple translation (or "shift") occurs. For example, if the closest SDR pixel is 100 m away from the GTM grid point, the data is moved 100 m during the production of the EDR files. There is no attempt to modify or adjust the data to account for this shift. This shift should always be less than the width of the SDR pixel and should not introduce significant errors.

Because the GTM grid is defined with constant spatial resolution and contains a constant number of pixels in the along-track and across-track dimensions, the spatial area represented by each EDR granule is constant. However, the spatial area represented by each SDR granule is not constant. The satellite orbit is not a perfect circle and the Earth is not a sphere, so the width of each scan as projected onto the Earth's surface varies as the distance between the Earth and the satellite varies from perigee to apogee. In addition, due to orbital mechanics, the satellite does not travel at a constant speed. Therefore, the distance in the along-track dimension of each SDR granule also varies between perigee and apogee.

The EDR granules are "maximized," meaning the width of the EDR granules (across-track dimension) is set to the maximum across-track distance possible in the SDR granules. Similarly, the length (along-track dimension) of the EDR granules is set to the maximum possible along-track distance in the SDR granules. This means that each EDR granule contains points on the GTM grid that are outside the bounds of the SDR data. These points are set to either the N/A fill value or the VDNE fill value.

Figure 15 shows an example of an EDR granule with fill values highlighted. This particular granule contained 18 rows of pixels at the end of the data arrays with the VDNE fill value. The associated EDR geolocation file for this granule also contains 18 rows of VDNE fill value at the end of the arrays. There are a varying number of pixels in each row (on either edge) that are given N/A fill value in the data file. In contrast, these pixels contain valid (non-fill) latitude and longitude values. When plotting consecutive EDR granules, the rows of VDNE fill value must be removed from the arrays for the data to be properly displayed. When these rows of fill values are removed, the granules may be stitched together and will have no apparent "seam" at the granule boundaries, no gap between granules and no loss of spatial resolution. EDR files created prior to August 2013 use only N/A fill in these rows.

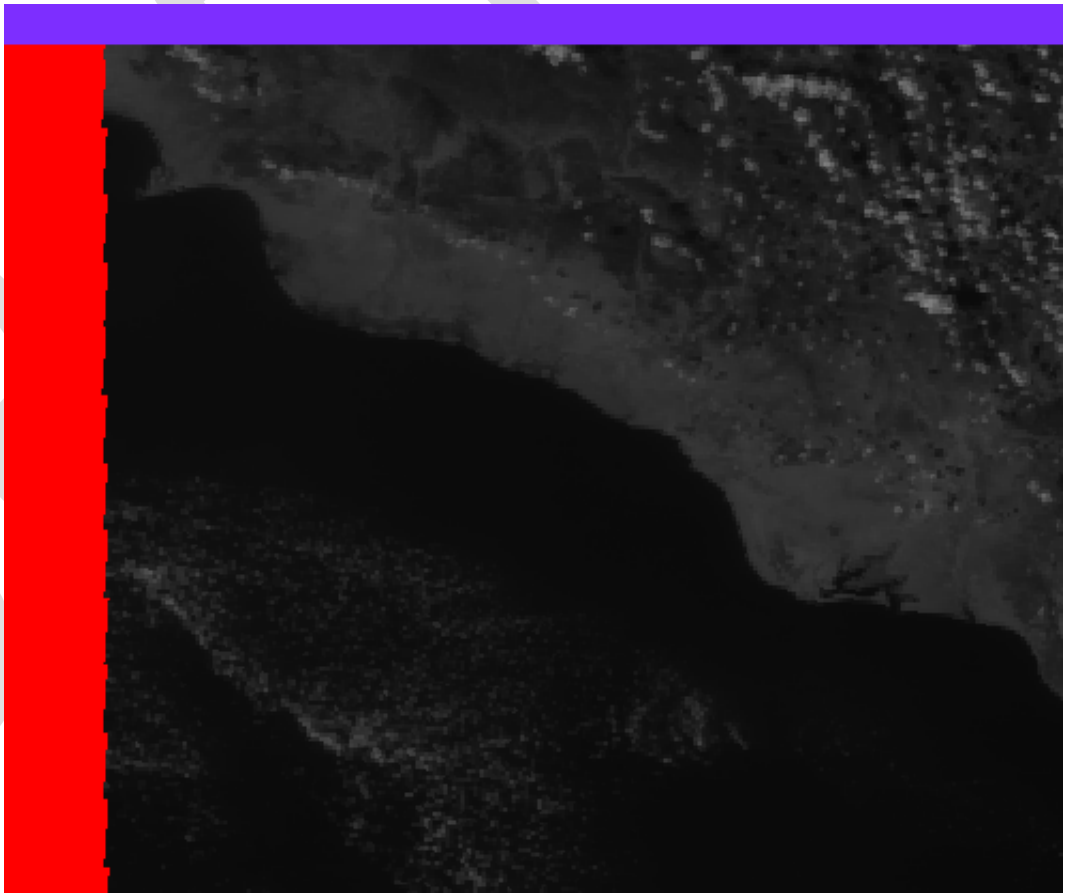

Figure 15. Example images of an EDR granule with fill values highlighted. These images were created from the I2 EDR granule with a start time of 08:14:21.9 UTC 24 October 2013 and have not been mapped to the Earth's surface. VDNE fill values are highlighted as purple in color, while N/A fill values are highlighted as red (see color scale below). Top: The full granule. Right: Zoomed in on the upper-left corner of the granule. Note the variable number of pixels in each row (that are beyond the edge of the VIIRS swath) given the N/A fill value.

The number of filled rows within the EDR arrays is a minimum at the Equator and increases as the satellite travels from the Equator to the poles. At the same time, the width of the filled area on the left and right edges of the array is greatest at the Equator and decreases toward the poles. This is shown schematically in Figure 16. During maneuvers of the S-NPP satellite, the center of the Earth-viewing portion of the scans may be off of satellite nadir (which is used to define the GTM grid). In this case, the area of N/A fill on the left and right edges of the affected granules will not be equal. In the NCC EDR data files, the area of N/A fill is typically not equal between the left and right edges of the granule.

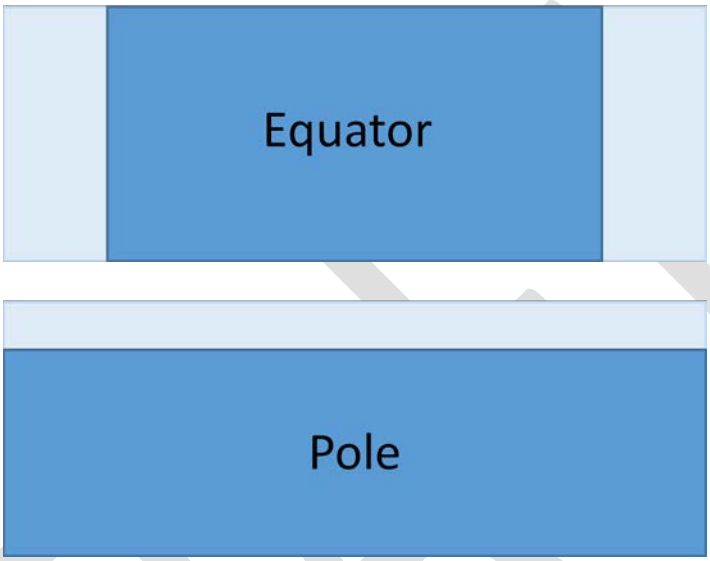

Figure 16. Exaggeration of the relative area of valid data within the area of an EDR granule, for granules near the Equator (above) and granules near the poles (below). The lightly shaded rectangles represent the area of fill values. The darker shaded rectangles represent the area of valid data.

6. The Day/Night Band SDR and Near Constant Contrast EDR

The Near Constant Contrast (NCC) EDR is the Imagery EDR based on the Day/Night Band (DNB) SDR. This EDR is unique, as it is not simply a remapping of the SDR data to the GTM grid. During the processing from the DNB SDR to the NCC EDR, the radiance values provided by the DNB are converted to a reflectance-like value, referred to as "pseudo-albedo" and recorded within the VNCCO files as the data array "albedo"[2]. Just as the SVDNB files contain only radiance values, VNCCO files contain only this pseudo-albedo. The primary purpose of the NCC EDR is to allow for the easy display of DNB data under all natural light conditions (sunlight,

[2] Because the DNB is sensitive to many more light sources at night than just reflected moonlight, the output of the NCC algorithm is not a true albedo. In particular, at night during a new moon, there is no reflected component of radiation from the moon. In that case, the primary sources of radiation detected by the DNB are emission sources.

moonlight and twilight). This section provides a brief overview of the purpose and process behind creating the NCC EDR.

The DNB is sensitive to radiance values ranging on the order of 10^{-2} W cm^{-2} sr^{-1} during daylight conditions to 10^{-10} W cm^{-2} sr^{-1} at night during a new moon. While the instrument is scanning across the day/night terminator, the observed radiance may vary by 7-8 orders of magnitude over the space of a single granule. This large dynamic range is difficult to display without saturation or losing detail at low end of the radiance scale, as many software display packages may only handle 256 colors. Figure 17 shows an example of a DNB granule near the day/night terminator and the associated NCC granule. By converting from radiance space to reflectance space, the dynamic range of the data to be displayed is reduced from 6-8 orders of magnitude to 1-3 orders of magnitude. This allows images to maintain a nearly constant contrast for scenes near the terminator and for nighttime imagery to appear similar to daytime imagery with minimal effort on the part of the user.

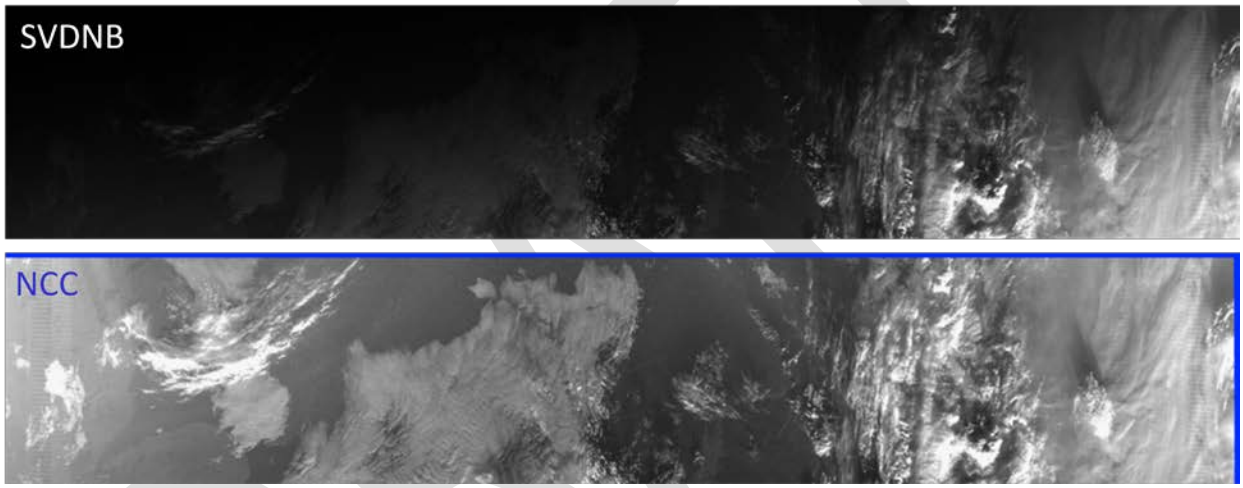

Figure 17. Example images produced from the DNB SDR (top) and NCC EDR (bottom) for a granule that straddles the day/night terminator. Fill values have been highlighted in blue.

For most visible wavelength channels (on VIIRS and other satellite instruments), the reflectance is the ratio between the incoming solar radiation incident on the Earth and the reflected radiation observed by the satellite. These channels do not provide valid data at night[3]. As the DNB is sensitive to nighttime radiation over the full lunar cycle, the incoming solar and lunar radiation must be properly modeled to calculate the reflectance. However, the DNB is sensitive to more sources of radiation than just the sun and moon.

The observed radiation at night typically varies over the magnitude range of 10^{-6} W cm^{-2} sr^{-1} during a full moon to 10^{-10} W cm^{-2} sr^{-1} during a new moon. While moonlight is not present during a new moon, “airglow” (the excitation of molecules in the upper atmosphere due to interactions with ultraviolet radiation resulting in the emission of photons) produces radiation that may approach 10^{-9} W cm^{-2} sr^{-1}. City lights may be as bright as 10^{-7} to 10^{-6} W cm^{-2} sr^{-1}. Auroras are commonly observed by the DNB at values from 10^{-9} to 10^{-7} W cm^{-2} sr^{-1}. The radiation produced by lightning and fires is highly variable, and may exceed that of city lights. It

[3] The M10 SDR files do contain valid data at night. This is to help with nighttime detection of fires.

is not possible to include the contributions of lightning, fires, auroras and city lights within the solar and lunar radiation models used to calculate the reflectance.

While it is possible to account for the contribution of airglow, it has not been done at the time of this writing. As a result, the clear-sky offsets used in the DNB SDR calibration are too large. When the DNB radiances are calculated during the production of the SDR files, these offsets are subtracted, which may result in negative radiance values being reported. These values are kept in the SDR files (i.e. not replaced with SOUB fill) even though negative radiances are physically impossible. Some physical features visible in DNB imagery would be lost if the negative values were excluded by the user. These negative radiance values from the SDR files show up as negative pseudo-albedo values in the NCC EDR. The impact of accounting for airglow during the DNB calibration is currently being explored. Accounting for airglow would add scientific value to the SDR files and remove negative radiances. On the other hand, it is expected that most users would then wish to remove the airglow signal from the imagery, as it would interfere with detection of other physical features and result in a general brightening of swath edges relative to the center of the swath.

The myriad light sources observed at night that are not modeled may emit several orders of magnitude more radiation than the amount of moonlight reflected off the Earth's surface, which is modeled. As a result, the pseudo-albedo values in the NCC EDR files may approach 100 – 1000 for some scenes. Prior to the NCC EDR achieving the "Provisional" level of maturity (August 2013), a threshold was set within the operational code limiting the pseudo-albedo values to a range of 0 to 5. This resulted in city lights, fires, and other bright features at night being replaced with SOUB fill for nights that were not near a full moon. This threshold has been reset to the range of -10 to 1000.

Users should also note that, in addition to the conversion from radiance to albedo, the DNB SDR data is also remapped to the GTM grid during the production of the NCC EDR data using the same methodology presented in Section 5. The GTM grid used in the NCC geolocation is the same as that used in the M-band EDR geolocation files.

7. Data Access

The ground processing system developed for the JPSS Program is referred to as the JPSS Common Ground System (JPSS CGS). The JPSS CGS is comprised of three primary components: the Command, Control and Communications Segment (C3S), the Interface Data Processing Segment (IDPS) and the Field Terminal Segment (FTS). C3S is responsible for controlling satellite operations (e.g. maintaining the orbit, performing routine hardware tests, etc.). IDPS is responsible for the operational production and release of JPSS data. FTS is responsible for the software required for the non-operational production of data from Direct Broadcast ground stations (also called field terminals). IDPS receives the raw data from the satellite through C3S and creates the RDR, SDR and EDR files.

The primary source responsible for the distribution of VIIRS data is the IDPS at NOAA/NESDIS. The NOAA/NESDIS facilities in Suitland and College Park, MD house the C3S and IDPS. This is the primary source for VIIRS data globally. The Air Force Weather Agency in Omaha, NE has served as a secondary IDPS, however, this site distributes data only to military users, and is currently planning to phase out their involvement in the operational production and release of VIIRS data. By the end of 2014, it is expected that NOAA/NESDIS will be the only location where the operational data is produced and distributed to the general scientific and operational communities.

NOAA/NESDIS currently provides data directly to the National Weather Service (NWS), the National Climatic Data Center (NCDC), and EUMETSAT. NCDC is responsible for archiving VIIRS data, which is made available through the Comprehensive Large Array-data Stewardship System (CLASS) website: http://www.class.ncdc.noaa.gov/. CLASS is the primary source for users to acquire VIIRS data from around the globe, and the CLASS archive is maintained from the point that each VIIRS SDR and EDR product achieved Beta-level maturity. Note that CLASS does not maintain an archive of M-band EDR files. SDR geolocation and data files, I-band and NCC EDR geolocation and data files, and many other non-Imagery EDR products (and their associated geolocation files) are archived. Both the ellipsoid and terrain-corrected versions of the SDR geolocation are available. Data are available for free once the user registers an account. To reduce the number of files that need to be distributed, CLASS aggregates 4 consecutive granules with geolocation (approximately 6 minutes of data) into a single file in HDF-5 format. These files may be prohibitively large for some users. Users have the option of de-aggregating the data into individual granules (and separating the geolocation information into its original files) when ordering the data. Ordering data may take anywhere from minutes to hours, depending on the size of the order. Typically, VIIRS data are available on CLASS within 8 hours of being downlinked from the satellite.

In order to improve the efficiency of distributing recent S-NPP data, CLASS has also set up a FTP site (ftp://ftp-npp.class.ngdc.noaa.gov/) for anonymous downloading of the last 90 days of available SDR and EDR data. The FTP site distributes large chunks of data as .tar files that do not use the same file naming convention of the HDF-5 files. Each .tar file is associated with an XML file of the same name that contains a list of the aggregated (4-into-1) granules in HDF-5 format included in the .tar file. These granules are not necessarily contiguous.

Operational VIIRS data produced by NOAA/NESDIS (including M-band EDRs) are also sent to the GRAVITE server. Users must request special access to the GRAVITE server and set up a user account. User accounts are typically only given to those individuals or groups that have direct involvement with the JPSS program. Scripts are available for the automated downloading of data in near-real time, with latency ranging from 2-7 hours. Data are only available for approximately 30 days. Applications for access to GRAVITE are available at http://www.star.nesdis.noaa.gov/jpss/ADL.php. Data are distributed as individual granules in the native HDF-5 format. This is the primary source for accessing M-band EDR data.

The PEATE server located at the University of Wisconsin-Madison (also called “Atmosphere PEATE”) is another source of VIIRS data; however, PEATE provides only SDR files. Data is distributed as individual granules in the native HDF-5 format. An easy-to-use search feature will provide shell scripts for automated downloading. Users are not required to register an account. PEATE maintains an archive of M-band and DNB SDR files dating back to January 2012. I-band

SDR files are only kept for 90 days. PEATE only distributes the terrain-corrected geolocation for I-band and M-band SDRs. The PEATE website is located at http://peate.ssec.wisc.edu/flo. An FTP site is also set up at ftp://peate.ssec.wisc.edu/allData/ingest/viirs/. The PEATE archive provides data from around the globe.

Sites for Direct Broadcast data continue to be installed around the globe. Direct Broadcast data are produced similarly to the heritage local receiving stations used during the NOAA POES program. An appropriate antenna and ground station hardware are required, as is the Algorithm Development Library (ADL) software package. The ADL software package is available for download at https://jpss-adl-wiki.ssec.wisc.edu/mediawiki/index.php/Main_Page. The University of Wisconsin-Madison has set up a ground station for Direct Broadcast which provides data for most of the United States. VIIRS files are provided through anonymous FTP at ftp://ftp.ssec.wisc.edu/pub/eosdb/npp/viirs/. Direct Broadcast data typically has much lower latency than other data sources (typically 30 – 90 minutes); however, data are only available for granules that are within the range of the antenna. The Wisconsin Direct Broadcast server provides SDR data and I-band Imagery EDR data from granules over the 48 contiguous United States and parts of Canada and only for the last seven days.

8. Data Display

The Community Satellite Processing Package (CSPP) made available by the University of Wisconsin-Madison is free, open source software that may be used to process Direct Broadcast data (i.e. create SDR files from Direct Broadcast RDR files), as well as process and display SDR files. Imagery EDRs are not currently supported. More information on CSPP may be found at http://cimss.ssec.wisc.edu/cspp/.

TeraScan software is another software package capable of producing SDR files from Direct Broadcast RDRs, as well as processing and/or displaying SDR data. Imagery EDRs are not supported, although several non-Imagery EDRs are. A license is required. More information about TeraScan may be found at http://www.seaspace.com/software.php.

As VIIRS SDRs and EDRs are distributed in the standardized HDF-5 format, any software package with routines capable of reading HDF-5 files may be used to process and/or display VIIRS Imagery data. Common software packages capable of reading HDF-5 files include IDL (http://www.exelisvis.com/ProductsServices/IDL.aspx), ENVI (http://www.exelisvis.com/ProductsServices/ENVI/ENVI.aspx), Matlab (http://www.mathworks.com/products/matlab/), HDF Viewer (http://www.hdfgroup.org/hdf-java-html/hdfview/) and McIDAS-V (http://www.ssec.wisc.edu/mcidas/software/v/). ENVI users may need the appropriate plug-in to read HDF-5 files. HDF Viewer only allows the display of images in data array space and does not have the capability to map the data to a projection of the Earth's surface. Various user groups have also developed Python routines to read and display VIIRS imagery.

9. Additional Resources

As this User's Guide was designed to serve as a brief overview of the VIIRS Imagery EDRs, users of this guide are encouraged to consult the additional information within the Algorithm Theoretical Basis Documents (ATBDs), Operational Algorithm Description (OAD) documents and Common Data Format Control Book (CDFCB) documents for the JPSS program. These documents, along with up-to-date instrument and data status documents and User's Guides for other JPSS products may be found online at http://www.star.nesdis.noaa.gov/jpss/ATBD.php.

The VIIRS Imagery and Visualization Team has set up a website at http://rammb.cira.colostate.edu/projects/npp/ where users will find items related to instrument or data issues, interesting imagery examples, and presentations given by various Team members.

Various user groups have also developed web-logs (blogs) that demonstrate the capabilities and uses of VIIRS data. Below is a list of blogs created by various NOAA and NASA cooperative institutes. This list is not intended to be comprehensive.

- http://rammb.cira.colostate.edu/projects/npp/blog/
- http://cimss.ssec.wisc.edu/goes/blog/archives/category/viirs
- http://rammb.cira.colostate.edu/projects/alaska/blog/
- http://nasasport.wordpress.com/category/viirs/
- http://goesrnatcentperspective.wordpress.com/category/viirs/

Various user groups have also set up websites for the display of VIIRS imagery in near-real time. Links to some of these websites are provided below.

- http://rammb.cira.colostate.edu/ramsdis/online/npp_viirs.asp
- http://www.nrlmry.navy.mil/VIIRS.html
- http://weather.msfc.nasa.gov/sport/jpsspg/viirs.html

Information on the calibration of VIIRS data may be found in Cao et al. (2013b,c). Additional calibration information is available at https://cs.star.nesdis.noaa.gov/NCC/VIIRS. The references below include additional articles in the refereed literature pertaining to VIIRS performance and calibration.

10. References

Bouali, M. and A. Ignatov (2013): Adaptive Reduction of Striping for Improved Sea Surface Temperature Imagery from Suomi National Polar-orbiting Partnership (S-NPP) Visible Infrared Imaging Radiometer Suite (VIIRS). *J. Atmos. Ocean Tech.*, in press, http://dx.doi.org/10.1175/JTECH-D-13-00035.1

Cao, C., F. DeLuccia, X. Xiong, R. Wolfe, F. Weng (2013c): Early On-orbit Performance of the Visible Infrared Imaging Radiometer Suite (VIIRS) onboard the Suomi National Polar-orbiting Partnership (S-NPP) Satellite, *IEEE Trans. on Geosci. and Remote Sens.*, in press, doi:10,1109/TGRS.2013.2247768

Cao, C., X. Shao, X. Xiong, S. Blonski, Q. Liu, S. Uprety, X. Shao, Y. Bai, F. Weng (2013b): Suomi NPP VIIRS sensor data record verification, validation, and long-term performance monitoring, *Journal of Geophysical Research: Atmospheres*, **118**, 11664-11678, doi:10.1002/2013JD020418

Cao, C., X. Xiong, R. Wolfe, F. DeLucca, Q. Liu, S. Blonski, G. Lin, M. Nishihama, D. Pogorzala, H. Oudrari, and D. Hillger (2013a): Visible Infrared Imaging Radiometer Suite (VIIRS) Sensor Data Record (SDR) User's Guide Version 1.2. *NOAA Technical Report NESDIS 142*, National Oceanic and Atmospheric Administration, Washington, D.C. 43pp.

Gao, B. and W. Chen (2012): Multispectral decomposition for the removal of out-of-band effects of visible/infrared imaging radiometer suite visible and near-infrared bands. *Applied Optics*, **51**, 4078-4086, http://dx.doi.org/10.1364/AO.51.004078

Hillger, D., T. Kopp, T. Lee, D. Lindsey, C. Seaman, S. Miller, J. Solbrig, S. Kidder, S. Bachmeier, T. Jasmin and T. Rink (2013): First-light Imagery from Suomi NPP VIIRS. *Bulletin of the American Meteorological Society*, **94**, 1019-1029, doi:10.1175/BAMS-D-12-00097.1.

Lee, T. F., S. D. Miller, F. J. Turk, C. Schueler, R. Julian, S. Deyo, P. Dills, and S. Wang, 2006: The NPOESS VIIRS Day/Night visible sensor. *Bull. Amer. Meteor. Soc.*, **87,** 191–199.

Liu, Q., C. Cao and F. Weng (2013): Assessment of Suomi National Polar-Orbiting Partnership VIIRS Emissive Band Calibration and Inter-Sensor Comparisons. *IEEE J. Selected Topics Appl. Earth Obs. Rem. Sens.*, **6**, 1737-1748, doi: 10.1109/JSTARS.2013.2263197

Liu, Q, C. Cao and F. Weng (2013): Striping in the *Suomi NPP* VIIRS Thermal Bands through Anisotropic Surface Reflection. *J. Atmos. Ocean Tech.*, **30**, 2478-2487, http://dx.doi.org/10.1175/JTECH-D-13-00054.1

Miller, Sh., K. Grant and J. J. Puschell (2013a): VIIRS Improvements Over MODIS. *2013 EUMETSAT Meteorological Satellite Conference and 19th AMS Satellite Meteorology, Oceanography and Climatology Conference*. Vienna, Austria, 16-20 September 2013.

Miller, St. D., W. Straka III, S. P. Mills, C. D. Elvidge, T. F. Lee, J. Solbrig, A. Walther, A. K. Heidinger and S. C. Weiss (2013b): Illuminating the Capabilities of the Suomi National Polar-orbiting Partnership (NPP) Visible Infrared Imaging Radiometer Suite (VIIRS) Day/Night Band. *Remote Sensing*, **5**, 6717-6766. doi:10.3390/rs5126717

Schueler, C. F., T. F. Lee and S. D. Miller (2013): VIIRS Constant Spatial-Resolution Advantages. *Int. J. Remote Sensing*, **34**, 5761–5777, http://dx.doi.org/10.1080/01431161.2013.796102

Uprety, S., C. Cao, X. Xiong, S. Blonski, A. Wu and X. Shao (2013): Radiometric Intercomparison between *Suomi-NPP* VIIRS and *Aqua* MODIS Reflective Solar Bands Using Simultaneous Nadir Overpass in the Low Latitudes. *J. Atmos. Ocean Tech.*, **30**, 2720-2736, http://dx.doi.org/10.1175/JTECH-D-13-00071.1

11. List of Acronyms

ADL	Algorithm Development Library
ATBD	Algorithm Theoretical Basis Document
AVHRR	Advance Very High Resolution Radiometer
C3S	Command, Control and Communications Segment
CDFCB	Common Data Format Control Book
CGS	Common Ground System
CLASS	Comprehensive Large Array-data Stewardship System
CSPP	Community Satellite Processing Package
DMSP	Defense Meteorological Satellite Program
DNB	Day/Night Band
EDR	Environmental Data Record
ENVI	Environment for Visualizing Images
EUMETSAT	European Organisation for the Exploitation of Meteorological Satellites
FTP	file transfer protocol
FTS	Field Terminal Segment
GRAVITE	Government Resource for Algorithm Verification, Independent Testing and Evaluation
GTM	Ground Track Mercator
HDF-5	Hierarchical Data Format version 5
HSI	horizontal sampling interval
IDL	Interactive Data Language
IDPS	Interface Data Processing Segment
JPSS	Joint Polar Satellite System
KPP	Key Performance Parameter
McIDAS	Man computer Interactive Data Access System
MODIS	Moderate-resolution Imaging Spectroradiometer
MSL	mean sea level
NASA	National Aeronautics and Space Administration
NCC	Near Constant Contrast
NCDC	National Climatic Data Center
NESDIS	National Environmental Satellite, Data, and Information Service

NIR	near-infrared
NOAA	National Oceanic and Atmospheric Administration
OAD	Operational Algorithm Description
OLS	Operational Linescan System
PEATE	Product Evaluation and Test Element
POES	Polar Orbiting Environmental Satellite
RDR	Raw Data Record
RGB	red-green-blue
RSR	relative spectral response
SDR	Sensor Data Record
S-NPP	Suomi National Polar-orbiting Partnership satellite
UTC	Coordinated Universal Time
VIIRS	Visible Infrared Imaging Radiometer Suite
WGS84	World Geodetic System 1984